Article

Quantitative Analysis of Fundus-Image Sequences Reveals Phase of Spontaneous Venous Pulsations

Fabrice Moret[1], Charlotte M. Reiff[1], Wolf A. Lagrèze[1], and Michael Bach[1]

Eye Center, University Medical Center, Freiburg, Germany

Purpose: Spontaneous venous pulsation correlates negatively with elevated intracranial pressure and papilledema, and it relates to glaucoma. Yet, its etiology remains unclear. A key element to elucidate its underlying mechanism is the time at which collapse occurs with respect to the heart cycle, but previous reports are contradictory. We assessed this question in healthy subjects using quantitative measurements of both vein diameters and artery lateral displacements; the latter being used as the marker of the ocular systole time.

Methods: We recorded 5-second fundus sequences with a near-infrared scanning laser ophthalmoscope in 12 young healthy subjects. The image sequences were coregistered, cleaned from microsaccades, and filtered via a principal component analysis to remove nonpulsatile dynamic features. Time courses of arterial lateral displacement and of diameter at sites of spontaneous venous pulsation or proximal to the disk were retrieved from those image sequences and compared.

Results: Four subjects displayed both arterial and venous pulsatile waveforms. On those, we observed venous diameter waveforms differing markedly among the subjects, ranging from a waveform matching the typical intraocular pressure waveform to a close replica of the arterial waveform.

Conclusions: The heterogeneity in waveforms and arteriovenous phases suggests that the mechanism governing the venous outflow resistance differs among healthy subjects.

Translational relevance: Further characterizations are necessary to understand the heterogeneous mechanisms governing the venous outflow resistance as this resistance is altered in glaucoma and is instrumental when monitoring intracranial hypertension based on fundus observations.

Introduction

Spontaneous venous pulsation (SVP) is a rhythmic variation in vein diameter observed ophthalmoscopically at the optic nerve head in 80% to 90% of subjects.[1,2] Its clinical relevance lies in differentiating early papilledema from pseudopapilledema[3,4] and it serves as a negative marker for intracranial pressure above 14 mmHg.[5] Lumbar puncture is considered to be more reliable than SVP monitoring[6] to rule out elevated intracranial pressure (ICP). Still, improved SVP monitoring could benefit subjects requiring regular or long term ICP monitoring.[7] Various associations have also been reported between SVP and glaucoma: (1) venous pulsation evoked by ophthalmodynamometry indicates higher venous pressure in glaucoma subjects,[8–10] (2) SVP incidence is lower in glaucoma,[11–14] (3) SVP is related to the severity of functional damage,[11,13,15,16] and (4) SVP is predictive of disease progression.[17–19] Obviously, SVP could be employed more efficiently if its etiology was better understood.

Understanding SVP etiology relies on a key point, namely when does venous collapse occur within the cardiac cycle? Since SVP was first observed, it has been reported that a collapse, partial or total, coincides with the systole.[20,21] Several hypotheses have been proposed based on this observation: (1) blood volume pulsation induces intraocular pressure (IOP) pulsation, occasionally overcoming intralumi-

nal venous pressure and thus collapsing veins,[21] (2) increased blood velocity during the systole induces intraluminal pressure reduction through the Venturi effect, leading to collapse,[22] (3) venous flow is constant while the IOP/ICP pressure-gradient pulsates, leading to translaminar pressure pulsation inducing collapse,[23] and (4) pulsation is a self-excited oscillation as observed in collapsible tube, mode-locking on external periodic pressure fluctuations when present.[24] The latter hypothesis does not require IOP or ICP pulsation: SVP occurs just because of the IOP/ICP pressure gradient. Self-excited oscillations can lead to collapse independent of the cardiac phase, or to pulse-synchronized pulsation at different phases. Hypothesis (1) was abandoned after IOP proved to be lower than venous pressure across the heart cycle in experiments on rats and cats[25,26] while (2) through (4) remain.

Recently, Kain et al.[27] presented experimental results showing collapse occurring at diastole and proposed that hypothesis (3) could explain the pulsation assuming an inversion of the pulsatile pressure gradient during the heart cycle, i.e., that the ICP pulsation amplitude would be larger than the IOP's. That study combined heart pulse synchronization with digital fundus imaging, thus allowing convenient replay of image sequences. Surprisingly, their results stand in opposition to previous observations, even to those using pulse-synchronized acquisition[28] or cinematographic imaging techniques.[29] Morgan et al.[30] further strengthened the latter view by showing that the minimal vein diameter occurs in phase with minimal ICP and IOP, and conclude that the collapse occurs simultaneously with the intraocular and intracranial diastole. Kim et al.[31] reached identical conclusions studying a large cohort.

We re-examine here the collapse timing quantitatively, using a newly developed method[32] allowing visualization of arterial and venous pulsations on fundus image sequences. The advantage of this technique is to yield both objective ocular systole markers and collapse times from the same images. Briefly, fundus image sequences are corrected for slow and saccadic eye movements, and dynamic non-pulsating features are filtered using a principal component analysis (PCA). We applied this technique to near-infrared image sequences recorded in 12 young healthy volunteers and computed quantitative pulsatility metrics from the processed image sequences.

Methods

Subjects

We analyzed fundus images acquired from the right eyes of 12 subjects, six men and six women, between 22 and 31 years of age, without known systemic or ocular pathologies and not taking potentially interfering medication. In our previous study,[32] we described pulsations in nine of these subjects (S1–S8 and S11). All subjects were screened for IOP (11–19 mmHg), had normal ocular findings on slit lamp, scanning laser ophthalmoscope (SLO), and optical coherence tomography (OCT) examinations, and had a decimal visual acuity greater than or equal to 1.0 in the examined eye. This research followed the tenets of the Declaration of Helsinki[33] and was approved by the local institutional ethics committee. The subjects provided written informed consent after a detailed explanation of the nature of the study and potential consequences.

Instrument

Image acquisition, preprocessing, and filtering were generally similar to that previously described.[32] We summarize these steps below, detailing differences to the previous study.

Near-infrared images were acquired with a SLO (Spectralis HRA+OCT, Heidelberg Engineering, Heidelberg, Germany), which we equipped with custom near-infrared pupil monitoring for alignment. Two sequences of at least 45 images each were acquired in each subject at a rate of 9 images/s. Drug-free mydriasis was achieved by dimming the ambient light. To partially standardize perfusion and ICP, subjects were seated at least 20 minutes prior to recording. We provide raw images as open data to promote reuse of the dataset[34,35] (see links in Supplementary Table S1 or the Dryad Digital Repository: http://dx.doi.org/10.5061/dryad.56f1h). The files are TIFF image stacks including 50 images of 386×768 pixels, coded on an eight-bit linear grayscale table.

Image Preprocessing

This step generates image sequences free of eye movements and instrumental artifacts. First the images were trimmed to a vertical band including the optic disk, to exclude the central light reflex of the SLO. Then the images were registered. Finally, the images distorted by microsaccades during their
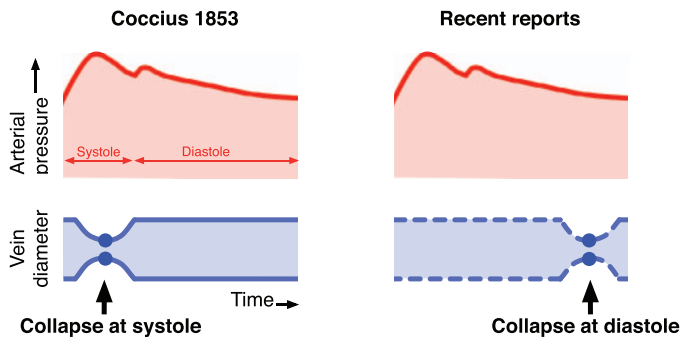
Figure 1. Schematized view of previous reports of collapse times in the cardiac cycle. The collapse time is important to understand the etiology of spontaneous venous pulsation. Coccius's report suggests a straightforward pressure-transfer effect of the systolic peak, while recent reports require a more complex model involving intracranial pressure.
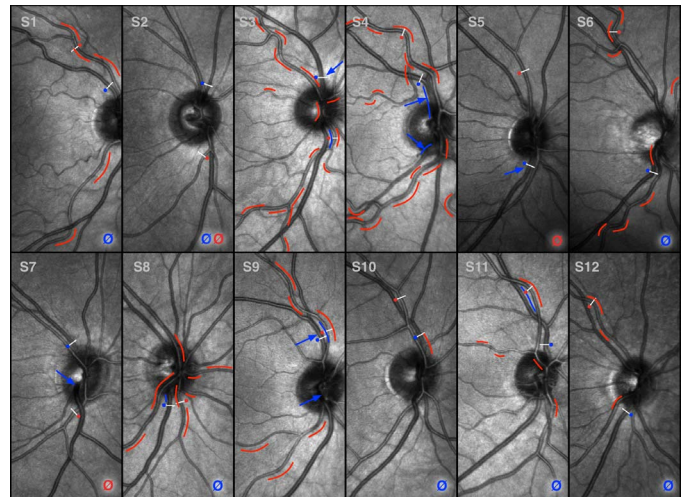

Figure 2. Measurement sites of lateral arterial pulsation used as reference for ocular systole (*white bars with red dots*) and measurement sites of diameters at spontaneous venous pulsation (*white bars with blue dots*) in the 12 subjects. When no SVP was observed, venous segments proximal to the disk were measured. Dots indicate the origin (zero) of profiles. Serpentine arterial pulsation (*red lines*) and spontaneous venous pulsation sites (*blue arrows*) or lack thereof (*empty-set symbols*) are indicated.

acquisition (on average less than 15%) were replaced by reconstructions synthesized from adjacent images in a fade-out fade-in fashion (see Supplementary Table S1 for online visualization of the movies). Finally all sequences were trimmed to 35 images to provide uniform input to the next step. The algorithms for preprocessing and all following analysis and visualization were implemented using Igor Pro 6.1 (WaveMetrics Inc., Lake Oswego, OR).

PCA Filtering and Pulsation Maps

We performed a PCA to segregate the various components of the image sequences and retained those coding the pulsations to create new image sequences largely free of noise or other distractors. The resulting sequences together with the preprocessed sequences can be visualized online (Supplementary Table S1). The PCA-filtered sequences allow to distinguish quite minute pulsations.[32] The most important are the SVP and the serpentine movement of the arteries. The serpentine movement is a lateral shift of the vessel, usually visible at bends. Waveform analysis of this movement suggested that it could serve as a marker of the arterial pressure waveform.[32] To prepare for the next step, each movie and the principal components were scrutinized and lateral pulsations (red lines bordering arteries on the systolic movement side) and SVPs (blue arrows) or lack thereof where indicated on a map (Fig. 2).

Vessel Metrics

Selection of Measurement Sites

We selected arteries showing the strongest lateral movements. Sites were typically chosen at the apex of the most curved and regular segments, and distant from arteriovenous crossings, branching, and neighboring vessels. If no serpentine pulsation was observable, we selected the most likely location where lateral pulsation might still be measurable. SVP was observed either inside or proximal to the optic disk. Measuring diameters inside the disk would require individually-customized algorithms, as the appearance of the vessels and their surroundings are highly variable. For subjects presenting an SVP inside the disk, we selected the first suitable site outside, but closest to the disk. We then measured intensity profiles at both arterial and venous sites (white bars in Fig. 2). The origins of the intensity profiles (dots in Fig. 2) were set such that a positive arterial excursion corresponds to a pressure increase. The vessel metrics were retrieved from both preprocessed and PCA-filtered image sequences to test for potential PCA-introduced artifacts:

Vessel Diameter (Venous)

To facilitate super-resolution analysis, the 10-pixel wide intensity profiles were upsampled 10× and low-pass filtered. A sliding linear regression filter,[36] adjusted for our near-infrared images, was applied to these intensity profiles to derive vessel metrics: first a sliding linear fit (20-pixels wide) was performed across the profile, yielding a smooth local slope. From the slope curve, the peaks and troughs were isolated
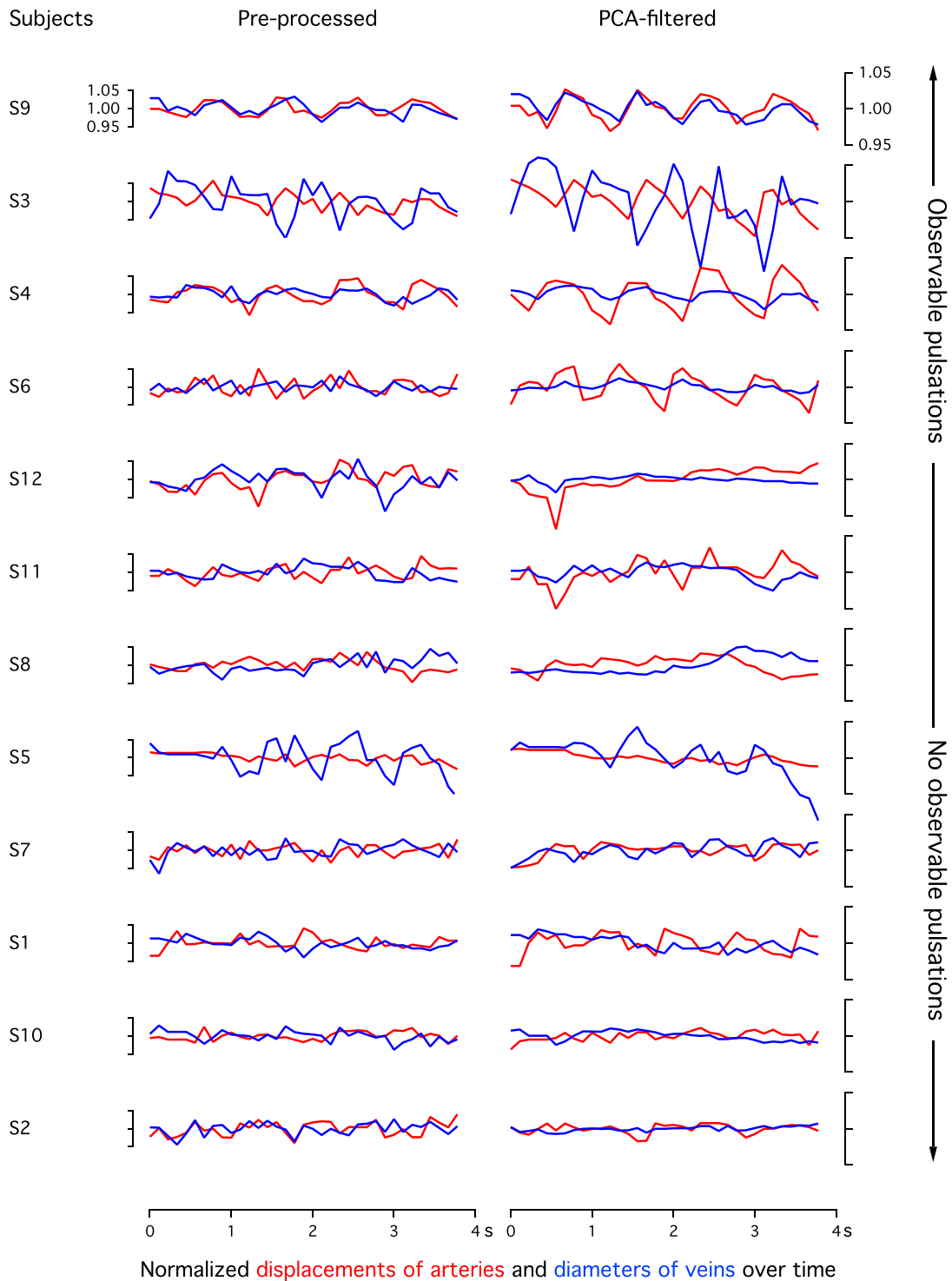
Figure 3. Arterial displacements (*red*) and venous diameters (*blue*) over time, normalized by average vessel diameters. Vessels metrics were measured on image sequences after preprocessing (*left*) and after additional PCA filtering (*right*). Comparing the two columns demonstrates that PCA filtering did not introduce artifacts. Noncollapsed/collapsed veins as described in Figure 1 were never observed; instead diameters display complex waveforms over time. The waveforms show different temporal relations, for example, in S3 troughs in the venous diameter signal coincide with arterial systolic peaks, whereas in S9, the venous diameter waveforms and arterial displacements (proxy for arterial pressure) are very similar in shape and without time delay.

by thresholding above and below half heights and depths; then the centroids of the remaining hills and valleys were calculated. The vessel diameter was defined as the distance between these centroids; its time course was measured across images.

Vessel Displacement (Arterial)

Displacement is change of position over time. Here, position was defined as the mean of the position of the two centroids defined above. Compared with other approaches (single-edge location, central reflex) this proved optimal in noise rejection and immunity to local vessel appearance variations.

Combined Visualization of Vessel Metrics

We normalized the lateral arterial displacement signals and venous diameter signals over the mean diameter of the temporal segment considered, and represented them jointly (Fig. 3). The sequence of subjects is organized from high (top) to low (bottom) subjective pulsation-detectability and factors-in simultaneous arteriovenous pulsations-availability and arteriovenous waveform temporal relations.

Results

Pulsations and Measurement Sites

Figure 2 shows the loci of lateral arterial pulsation and SVP on the fundi of the 12 subjects. Nine subjects presented serpentine pulsation and five SVP. Of the five subjects showing an SVP, one (S7) had an SVP only inside the disk, which required measuring venous diameter elsewhere; this SVP is particular as the pulsation is a movement of the segment diving into the optic nerve head rather than a change in diameter (also observed in S9). In S4, we could not measure the segment showing SVP outside of the disk due to the proximity of an artery, and thus measured farther away.

Figure 3 illustrates normalized arterial displacements (red) as an ocular arterial pressure surrogate, and venous diameters (blue) over time, after preprocessing and after additional PCA filtering. Comparison between preprocessed and PCA-filtered data revealed that filtering did not induce artifacts, thus corresponding waveforms were good for further analysis. Comparing the measured waveform to a typical waveform (fast systolic upslope and peak followed by a slower diastolic downslope, possibly with a dichrotic notch), revealed that PCA filtering improved the measured signals, at least in subjects S3, S4, S6, S9, revealing identifiable systole upslope

onsets. Overall, an arterial pulsation was usable as a time reference in seven subjects and a venous pulsation in eight. Four subjects presented both (S3, S4, S6, and S9) after PCA filtering, which allowed to investigate the temporal relation between venous pulsation and arterial ocular systole.

"Ideal" model behaviors (noncollapsed/collapsed) of veins, as illustrated in Figure 1, were never observed. Instead, we see complex waveforms. S3 and S9 displayed the extremes in terms of temporal relation to the ocular systole. In S3, troughs in the venous diameter signal coincide with arterial systolic peaks. In S9, venous diameter and arterial displacement waveforms are very similar and without time shift. In intermediate subjects (S4 and S6), the venous waveforms are more difficult to make out due to lower signal to noise ratio (SNR) or less radical waveforms. The venous signal in S4 seems to show a slight delay between the arterial and venous systolic upslope onsets, and a more rounded waveform with a slower peak and diastolic decay. S6 reveals sharper peaks and resembles S9.

Phase of Venous Collapse

The perception of the temporal relationship between arteriovenous signals may not be straightforward when the amplitude of the pulsations signals is represented after normalization by vessel diameter (Fig. 3). Figure 4 allows inference at glance of the relationship in those four subjects that show both clearly recognizable arterial and venous pulsations. We normalized the PCA-filtered signals by peak-to-peak amplitude, after applying linear detrending (Fig. 4, left column). Systole onsets (Fig. 4, red diamonds) were detected automatically based on positive inflections processed over two points, and served to build pulse-averaged signals (Fig. 4, right column). This process allows classifying subjects by arteriovenous relationships as represented here from in- to out-of-phase.

Objective Quantification of Arteriovenous Delays

While phase relationships can be already visually inferred after applying appropriate signal processing and visualization methods (Fig. 4), objective and statistically testable quantification is necessary to pave the way for clinical studies. Arteriovenous lags are quantified by cross-correlation (Fig. 5, right column, peak tags) coupled with a 100,000-permutations Monte-Carlo significance test (Fig. 5, right
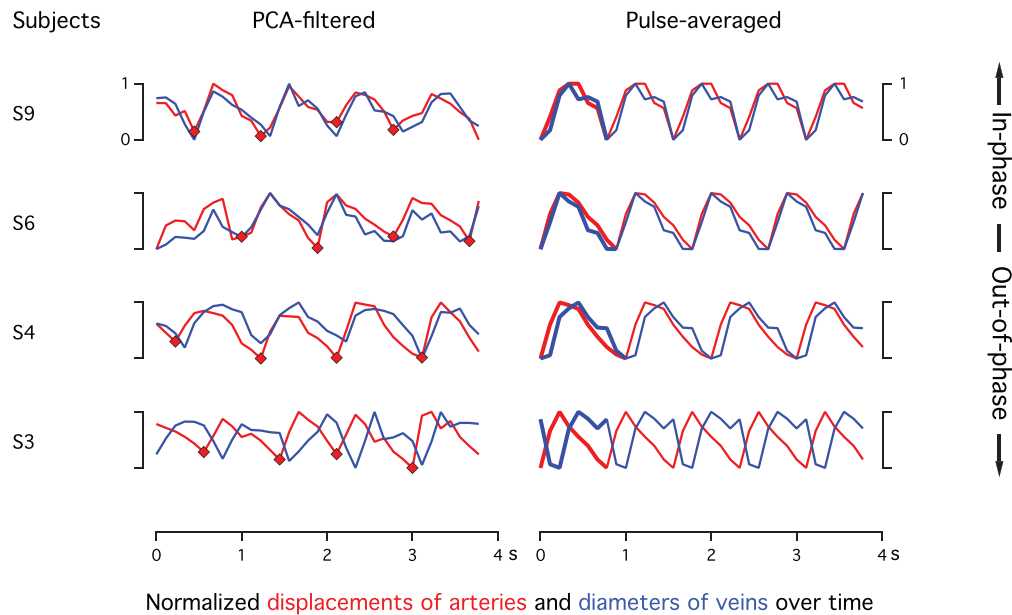
Normalized displacements of arteries and diameters of veins over time

Figure 4. Signals from four subjects (S6, S9, S4, S3) from Figure 3 showing clearly recognizable arterial and venous pulsations. The *left column* depicts the PCA-filtered signals. The systole onsets have been detected automatically, indicated by *red diamonds*. The *right column* shows pulse-averaged arteriovenous signal cycles based on these references and repeated for another three cardiac cycles. All signals are normalized peak-to-peak. The pulse-averaged signals allow inferring the temporal arteriovenous relationship at a glance. Based on this, subjects are ordered from in-phase (*top*) to out-of-phase (*bottom*). S6 and S9 show closely matching arteriovenous signals, S4 a slightly delayed venous signal and S3 counter-phased signals.

column, two-tailed envelopes at $P = 0.001$ in gray). The position of the peaks (labeled in the figure) shows, respectively, 0, 0, 0.11, and 0.22-s delays for S9, S6, S4, and S3. All delays are significant with P values below 0.001, indicating that the observed arteriovenous phase differences are not due to noise but genuinely physiologic.

Test-Retest

To assess stability of the temporal relations found per subject, we ran re-tests on the two subjects at opposing ends of the waveform relations. Figure 6 shows that the relations remain constant over 10 minutes, in spite of poorer SNR; simplified: in-phase in S9, out-of-phase in S3. Arteriovenous delays for test-retest are: 0/0 s for S9 and 0.22/0.22 s for S3. All four metrics are statistically significant ($P < 0.001$) and confirm the intersubject heterogeneity in arteriovenous delays.

Pulse Wave Propagation Along Arteries?

A pressure change in a vessel propagates at a finite velocity: the pulse wave velocity (PWV). PWV in ocular circulation can be measured through diameter changes, but results differ widely.[37–40] We compared lateral pulsatile displacement waveforms at several sites along arteries. As previously, we chose locations with strong lateral displacement (i.e., at curve apexes). Figure 7 illustrates simultaneous arterial lateral displacement signals in subjects S3 and S9. We observed no delay between signals within our present time resolution. This validates arterial displacements as a temporal reference for ocular systole pressure, and differs from the findings of a recent study[40] reporting particularly slow values: for example, in young healthy patients, approximately six pulse pressure waves would travel over a retinal artery segment of 2 mm at normal heart rate. Additionally, arterial diameter signals at the measured locations (gray signals in Fig. 7) demonstrated systematically lower SNR than lateral displacements signals.

Discussion

Dynamic measurements of lateral arterial displacements and venous diameters at the site of SVP or near the disk from a fundus image sequence were obtained in four subjects. We found that the pulsating diameter of veins is not "either open or collapsed." Venous waveforms differ between healthy subjects, and demonstrate differing temporal relations to the ocular systole.
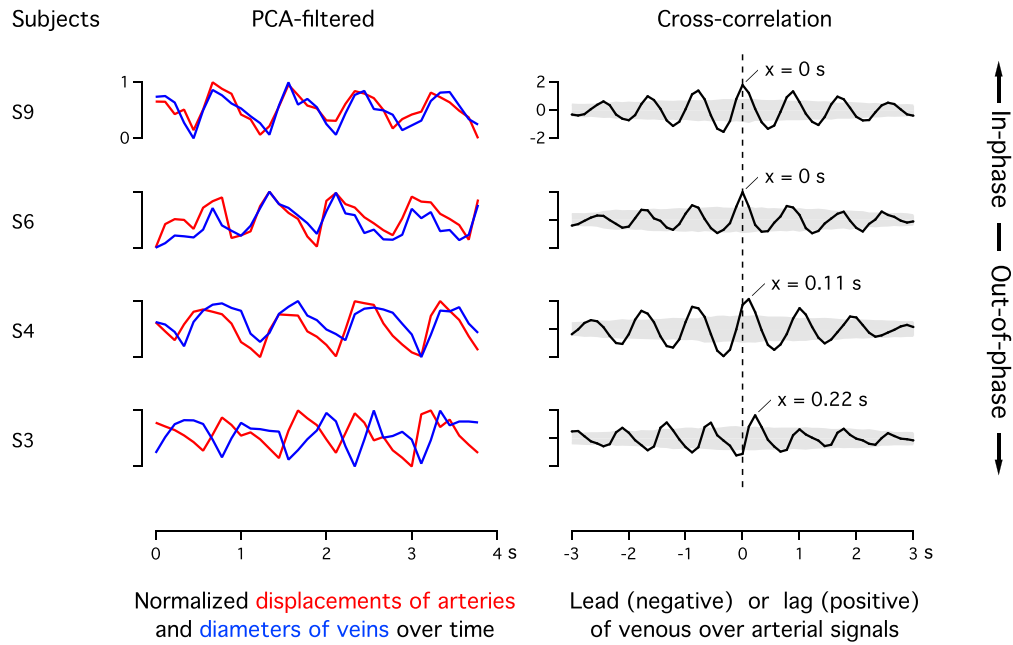
Figure 5. Signals from Figure 4 (*left column*) and corresponding cross-correlations of the arteriovenous signals. On the latter, the positions of the central peaks are either at zero (S6 and S9) or showing a slight lag of the venous signal over the arterial signal (S4: one-point lag = 0.11 s, S3: two-points lag = 0.22 s). All central peaks are statistically significant: theirs amplitude exceed the $P = 0.001$ two-tailed envelopes (*gray*) computed with a 100,000-permutations Monte-Carlo significance test. This quantitatively confirms the visual aspect on the previous signals.
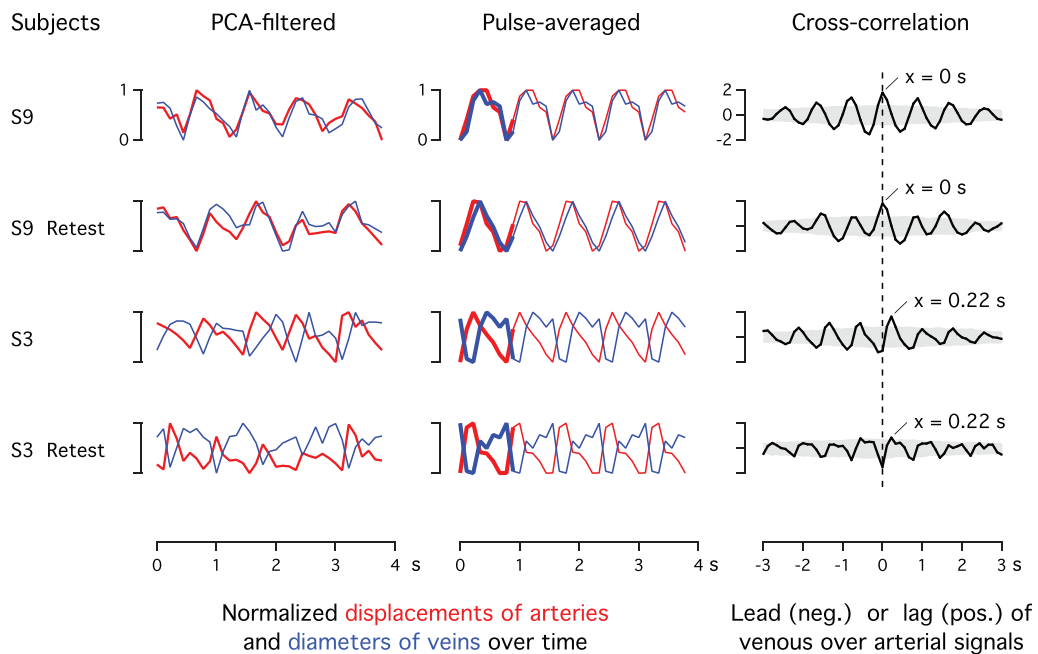

Figure 6. Test-retest assessment for two subjects with markedly different waveform relationships; *left column*: PCA-filtered trace, *central* and *right columns*: corresponding pulse-averages and cross-correlograms. The *top subject* (S9) shows a stable in-phase relationship between vein diameter (*blue*) and artery displacement (*red*) for the first test (*top*) and retest (10 minutes later, *below*). Subject 3 (*bottom traces*) shows an out-of-phase relationship.
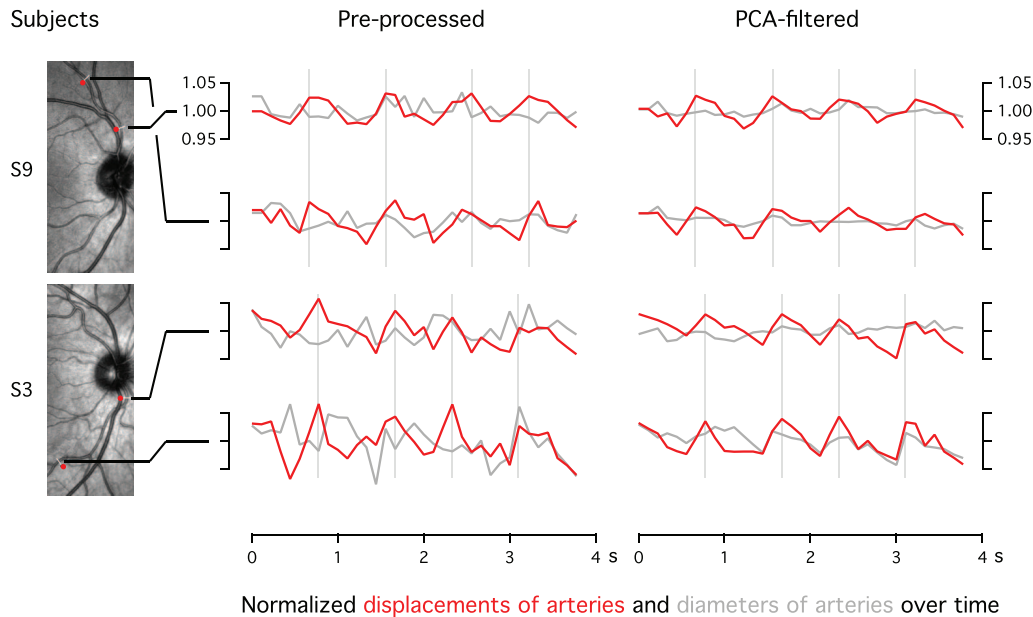
Figure 7. Waveforms for two sites of the same artery (indicated by *white bars* on fundus images at the *left*) for subjects 3 and 9. Artery displacements (*red*) show no delay between the two sites, indicating rapid pulse wave propagations in both subjects; thus, arterial displacements can function as time reference irrespective of measurement sites. Displacements (*red*) appear more appropriate as timing reference here than diameters (*gray*), given their higher signal-to-noise ratio.

Advantages of the Present Approach

Initial studies investigating the "time of collapse" were based on subjective ophthalmoscopic observations and remained controversial for decades.[41] Imaging[29,41] and, later, heartbeat-synchronized imaging[28] provided more objective and quantitative observations, but still relied on remote references such as electrocardiogram or peripheral pulse oxymetry for synchronization. The present method retrieves simultaneously (1) a local systolic time reference from the arterial pulsation[32] when available, and (2) vein metrics, via the same technique and from the same image sequence. Our measurements yield continuous, quantitative, and objective values without visual classification.[27,30,31] The comfort of patients is maximized by use of near-infrared light illumination and noncontact measurements. This enables long recordings and does not interfere with IOP. Finally, preprocessed and PCA-filtered sequences yield local pulse-onset times, thus not necessarily relying on nonlocal analysis such as Fourier or correlation techniques.[38,39]

Limitations

Compared with previous reports,[27,30,31,42] this study enrolled relatively young individuals. With increasing age, arterial pressure waveforms will change due to stiffening of the arterial walls, thus a generalization to pathophysiological situations typically related with age would benefit from observations in older subjects.

SLO imaging is limited to top-view observable vessel segments. A first consequence is that deeper venous pulsations within the optic nerve head may be missed.[43] A second consequence is that the shape of the vein cross-section remains unknown. As the transmural pressure decreases, the cross-section of an initially fully inflated vein will undergo shapes of a radially extended circular section, an ellipsoidal section, a dumbbell-like section, a dumbbell with contacting walls, peripheral bulbs joined by a central line where walls contact, and finally a fully collapsed line. Without the circular state, the apparent diameter of a vessel of undetermined cross-section may not be representative of the intraluminal section. Coherence-based techniques may overcome these two barriers.[44–46]

Regarding the localized nature of SVP, while many reports assumed a constant venous flow upstream to the SVP site, pulsation has been observed using various techniques.[45,47–50] Clearly, the constancy of the pulsation waveform along primary veins requires further study. We found that waveforms differ markedly between subjects; hence, a higher temporal resolution for better characterization should be sought in future investigations.
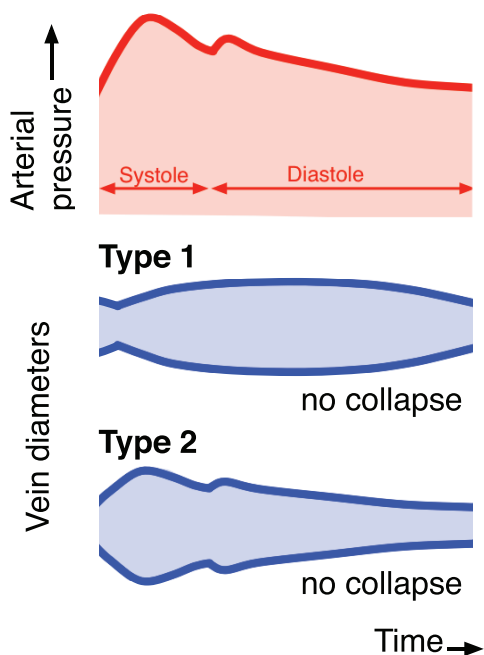
Figure 8. Schematized signals of diameter pulsations, illustrating that no binary "collapse" occurs; rather, diameters show continuous variation: Type 1, (e.g., subject 3), suggests a Windkessel effect. In contrast, Type 2 (e.g., subject 9) suggests a direct arteriovenous pressure transfer. Clearly, these interindividual variations imply different mechanisms at play.

Venous Waveforms Differ Among Subjects

The initial aim of this study was to determine the time at which veins collapse in the cardiac cycle. As we observed no temporally localized "collapse" (partial or total), diameter minima were considered. The timing of venous-diameter minima observed here shows two extreme behaviors as illustrated in Figure 8: in "type 1," minima coincide with arterial systolic upslopes, as in S3; and in "type 2," minima coincide with the end of arterial diastoles (or systolic upslope onsets), as in S9. These extreme types of minima, coinciding both with systolic time segments in some subjects, and diastolic time segments in others, reconciles previous contradictory studies supporting only one or the other. As discussed below, each type calls for a specific model to explain the respective waveform shapes. Intermediary cases, such as S4, may present a more moderate contribution of a single mechanism, or contributions from both mechanisms.

Type 1: Venous Pulsations as Windkessel Waveforms?

The venous diameter waveforms in S3 (Fig. 3) resemble the typical IOP pulsation waveform as produced by the uveal Windkessel effect (elastic storage and resistive outflow).[51,52] This waveform (Fig. 8, Type 1) is a dampened, low-pass filtered version of the choroidal arterial pressure, presenting a slower upslope and a later and more rounded peak. Of relevance here, the later upslope onset begins approximately halfway of the arterial systolic up-slope.

The resemblance of venous waveforms to typical IOP waveforms suggests some causal relationship. One explanation may be that the IOP pulsation is partially transferred to the venous pressure. A downstream modulation of the outflow resistance by the IOP has indeed been postulated, mediated, e.g., by IOP evoked deformation of the lamina cribrosa.[23] This is not supported by the observed correlation between the retrobulbar velocity and IOP waveforms.[53] This correlation suggested to those authors a dependence of the velocity over the IOP, and that outflow resistance remains constant throughout the pulse cycle in the subject shown.[53] Until this has been observed in more subjects, the hypothesis of an outflow resistance modulated by IOP should be retained. This hypothesis may explain the relationship between venous pulsations and ICP pulsations.[30] Without considering any causality of the second over the first; instead, the cerebral arterial waveform may be acting as the "hidden variable" and affect both IOP and ICP pulsation. While the ICP is not necessary in this hypothesis to explain lamina cribrosa resistance change, it may be involved as well, by contributing to modulate the translaminar pressure.[54]

The localized nature of the pulsation added to the fact that the pulsation appears as a partial collapse support a fast reduction of the downstream resistance. Beside a possible modulation of the lamina cribrosa resistance, further downstream segments may present resistance variations due to exposition to surrounding ICP pulsation, such as invoked by Levine[23] or Morgan.[30] The pulsation waveform of the ICP also depends on a Windkessel effect, and thus could also explain the observed waveform.

The pulsation may not be solely attributed to the aforementioned mechanisms. Additional local or catalytic factors already hypothesized may be at play here, e.g., a local decrease in vessel stiffness due to change in vessel curvature or surrounding tissues,[5] or the rhythmic collapse occurring in a Starling resistor system.[55] The latter can potentially phase-lock on small up- or down-stream resistance pulsations, for example, due to IOP (direct effect on vessel or indirect effect on lamina cribrosa) and/or due to ICP.

Considering the presently highly underdetermined situation, it is likely that the mechanisms generating the pulsation will only be firmly identified using techniques providing comprehensive data along the venous flow, starting from the orbital microcirculation, through the laminar region, to the retro-orbital circulation and maybe further downstream, at high temporal resolution, and coupled with additional information on local tissue stiffness and external pressures (IOP/ICP).

Type 2: Matched Arteriovenous Waveforms (Subject S9)

Subject S9 shows a very close match between the arterial and venous waveforms. This indicates (1) good reliability of measurements, and (2) implies a pulsation etiology differing from Type 1.

The close waveform match is a marker of reliability considering that: (1) the two metrics differ: a lateral displacement for one and a diameter in the other, and thus are not prone to the same imaging related artifacts, (2) the peak-to-peak amplitude of the signals covers approximately 11 μm or approximately the width of 2 pixels, and (3) the measured objects, a vein and an artery, are of different nature.

The waveforms closeness leads us to hypothesize that, in S9, the venous pulsation originates through a direct modulation of the outflow resistance by the arterial pressure. Indeed, any intermediary element in the causal chain linking the arterial pressure to the venous pressures would likely disrupt the tight match observed. Such modulation can occur from two of the following already hypothesized mechanisms. First, a transfer through a common adventitia[56–58]: As the central artery and central vein share a common rigid adventitial sheath inside the optic nerve, and as the arterial pressure rules over the venous pressure, the pulsating inflation of the artery will reduce the section available to the vein; this will lead to a pulsating outflow resistance, in turn affecting the upstream venous pressure. Second, a transfer through arteriovenous crossings[59]: where veins and arteries cross each other's nearby or inside the disk, leading to a pressure transfer. In both cases, fast coherence-based techniques allowing measuring the flow and diameter along vessels coursing through the optic nerve head, and retrobulbar color Doppler imaging may help identify the mechanism involved in the future.

Subject S9 presents no clinical finding but his peculiar venous pulsation raises the question whether it represents an early sign of congestion, as possibly in glaucoma or in central retinal vein occlusion, where such mechanisms have already been proposed.[60,61] Interestingly, arteriovenous waveforms presented recently by Morgan et al.[62] and measured in glaucomatous patients show a similar matching (data of Figure 3d after additional peak-to-peak normalization).

Arterial Pulsation Not Necessarily a Pathophysiological Sign

The arterial pulsation is used in this study as a marker of systole onset. Meanwhile, its high prevalence observed here calls for a side remark. Various pathologic conditions may lead to ophthalmoscopically observable retinal arterial pulsation: ocular ischemic syndromes,[63] aortic regurgitation (Becker's sign),[64] hyperthyroidism, and when the IOP is higher than the diastolic but lower than systolic blood pressure.[65] As Keyes and Hatcher[66] pointed out in 1940, arterial pulsation is not necessarily pathologic; indeed we observed it in 9 of 12 healthy young volunteers. This high prevalence certainly relates to the ideal fundus recording conditions (clear ocular media, ideal fixation, and subject compliance) and the improved observations allowed by the image processing. As new retinal imaging techniques disseminate steeply, arterial pulsations will be observed increasingly frequently. Thus, the so far implicit instrument for observing this feature, the ophthalmoscope, should now be mentioned when describing arterial pulsations as a "highly suggestive"[63] or "definitive"[67] sign of diseases. Also seen in textbooks, the description of the "presence of an arterial pulsation" alone is misleading; while an "increased arterial pulsation" would be more appropriate while waiting for quantitative studies.

Conclusions

Fundus sequences recorded with a clinical SLO and processed to reveal vessel pulsations enabled us to simultaneously appraise the pulsation waveforms of retinal artery displacements and vein diameters as markers of arterial ocular systole and venous retinal pulsation pressures, respectively. Marked differences of waveforms among healthy patients reveal the need for time-course recording to quantify the venous pulsation and its temporal relationship with the intraocular arterial systole. The intersubject variation in venous pulsation waveforms implies that the venous outflow resistance, a bottleneck in retinal

circulation though to be involved in various ocular pathologies, is likely governed by various mechanisms.

References

1. Harder B, Jonas JB. Frequency of spontaneous pulsations of the central retinal vein. *Br J Ophthalmol*. 2007;91:401–402.
2. Legler U, Jonas JB. Assessment of the spontaneous pulsations of the central retinal vein in daily ophthalmic practice. *Clin Experiment Ophthalmol*. 2007;35:870–871.
3. McCulley TJ, Lam BL, Bose S, Feuer WJ. The effect of optic disk edema on spontaneous venous pulsations. *Am J Ophthalmol*. 2003;135:706–708.
4. Jacks AS, Miller NR. Spontaneous retinal venous pulsation: aetiology and significance. *J Neurol Neurosurg Psychiatr*. 2003;74:7–9.
5. Levin BE. The clinical significance of spontaneous pulsations of the retinal vein. *Arch Neurol*. 1978;35:37–40.
6. Wong SH, White RP. The clinical validity of the spontaneous retinal venous pulsation. *J Neuro-ophthalmol*. 2012;33:17–20.
7. Golzan SM, Avolio A, Graham SL. Hemodynamic interactions in the eye: a review. *Ophthalmologica*. 2012;228:214–221.
8. Jonas JB. Central retinal artery and vein collapse pressure in eyes with chronic open angle glaucoma. *Br J Ophthalmol*. 2003;87:949–951.
9. Stodtmeister R, Ventzke S, Spoerl E, et al. Enhanced pressure in the central retinal vein decreases the perfusion pressure in the prelaminar region of the optic nerve head. *Invest Ophthalmol Vis Sci*. 2013;54:4698–4704.
10. Pillunat KR, Ventzke S, Spoerl E, Furashova O, Stodtmeister R, Pillunat LE. Central retinal venous pulsation pressure in different stages of primary open-angle glaucoma. *Br J Ophthalmol*. 2014;98:1374–1378.
11. Morgan WH, Hazelton ML, Azar SL, et al. Retinal venous pulsation in glaucoma and glaucoma suspects. *Ophthalmology*. 2004;111:1489–1494.
12. Legler U, Jonas JB. Frequency of spontaneous pulsations of the central retinal vein in glaucoma. *J Glaucoma*. 2009;18:210–212.
13. Abegao Pinto L, Vandewalle E, De Clerck E, Marques-Neves C, Stalmans I. Lack of spontaneous venous pulsation: possible risk indicator in normal tension glaucoma? *Acta Ophthalmol*. 2012;91:514–520.
14. Seo JH, Kim TW, Weinreb RN, Kim YA, Kim M. Relationship of intraocular pressure and frequency of spontaneous retinal venous pulsation in primary open-angle glaucoma. *Ophthalmology*. 2012;119:2254–2260.
15. Morgan WH, Balaratnasingam C, Hazelton ML, House PH, Cringle SJ, Yu D-Y. The force required to induce hemivein pulsation is associated with the site of maximum field loss in glaucoma. *Invest Ophthalmol Vis Sci*. 2005;46:1307–1312.
16. Kim M, Kim TW, Weinreb RN, Lee EJ, Seo JH. Spontaneous retinal venous pulsation and disc hemorrhage in open-angle glaucoma. *Invest Ophthalmol Vis Sci*. 2014;55:2822–2826.
17. Balaratnasingam C, Morgan WH, Hazelton ML, et al. Value of retinal vein pulsation characteristics in predicting increased optic disc excavation. *Br J Ophthalmol*. 2007;91:441–444.
18. Morgan WH, Hazelton ML, Balaratnasingamm C, et al. The association between retinal vein ophthalmodynamometric force change and optic disc excavation. *Br J Ophthalmol*. 2009;93:594–596.
19. Graham SL, Butlin M, Lee M, Avolio AP. Central blood pressure, arterial waveform analysis, and vascular risk factors in glaucoma. *J Glaucoma*. 2013;22:98–103.
20. Coccius E. *Ueber die Anwendung des Augen-Spiegels, nebst Angabe eines neuen Instrumentes*. Leipzig: Immanuel Müller; 1853.
21. Van Trigt AC. The ophthalmoscope. *Lancet*. 1853;2:417.

22. Williamson-Noble F. Venous pulsation. *Trans Ophthalmol Soc UK*. 1952;72:317–326.

23. Levine DN. Spontaneous pulsation of the retinal veins. *Microvasc Res*. 1998;56:154–165.

24. Baurmann M. Über die Entstehung und klinische Bedentung des Netzhautvenenpulses. *Dtsch Ophthalmol Ges*. 1925;45:53–59.

25. Duke-Elder WS. The venous pressure of the eye and its relation to the intra-ocular pressure. *J Physiol*. 1926;63:409–418.

26. Attariwala R, Giebs CP, Glucksberg MR. The influence of elevated intraocular pressure on vascular pressures in the cat retina. *Invest Ophthalmol Vis Sci*. 1994;35:1019–1025.

27. Kain S, Morgan WH, Yu D-Y New observations concerning the nature of central retinal vein pulsation. *Br J Ophthalmol*. 2010;94:854–857.

28. Bailliart P. Quelques considérations sur la pression dans la veine centrale de la rétine. *Ann Ocul*. 1931;168:513–539.

29. Swan KC, Bailey PF. Cinematography of the retinal vessels. *Trans Am Ophthalmol Soc*. 1959;57:210–220.

30. Morgan WH, Lind CR, Kain S, Fatehee N, Bala A, Yu DY. Retinal vein pulsation is in phase with intracranial pressure and not intraocular pressure. *Invest Ophthalmol Vis Sci*. 2012;53:4676–4681.

31. Kim M, Lee EJ, Seo JH, Kim TW. Relationship of spontaneous retinal vein pulsation with ocular circulatory cycle. *PLoS One*. 2014;9:e97943.

32. Moret F, Poloschek CM, Lagreze WA, Bach M. Visualization of fundus vessel pulsation using principal component analysis. *Invest Ophthalmol Vis Sci*. 2011;52:5457–5464.

33. World Medical Association. Declaration of Helsinki: ethical principles for medical research involving human subjects. *59th General Assembly, Seoul*. 2008.

34. Molloy JC. The Open Knowledge Foundation: open data means better science. *PLoS Biol*. 2011;9:e1001195.

35. Walport M, Brest P. Sharing research data to improve public health. *Lancet*. 2011;377:537–539.

36. Chapman N, Witt N, Gao X, Bharath AA, Stanton AV, Thom SA, Hughes AD. Computer algorithms for the automated measurement of retinal arteriolar diameters. *Br J Ophthalmol*. 2001;85:74–79.

37. Otto TP. Parametrization of the retinal blood flow by analysis of motion compensated angiography image sequences. Heidelberg, Germany: Ruprecht-Karl-Universität; 2000. Thesis.

38. Gugleta K, Kochkorov A, Katamay R, Zawinka C, Flammer J, Orgul S. On pulse-wave propagation in the ocular circulation. *Invest Ophthalmol Vis Sci*. 2006;47:4019–4025.

39. Kotliar KE, Baumann M, Vilser W, Lanzl IM. Pulse wave velocity in retinal arteries of healthy volunteers. *Br J Ophthalmol*. 2011;95:675–679.

40. Kotliar KE, Lanzl IM, Hanssen H, Eberhardt K, Vilser W, Halle M, Heemann U, Schmidt-Trucksass A, Baumann M. Does increased blood pressure rather than aging influence retinal pulse wave velocity? *Invest Ophthalmol Vis Sci*. 2012;53:2119–2126.

41. Serr H. Zur Analyse der spontanen Pulserscheinungen in den Netzhautgefässen. *Graefes Archiv für Ophthalmol*. 1937;137:488–505.

42. Weinstein P, Forgacs J. Circulatory studies of the fundus of the eye. *Br J Ophthalmol*. 1947;31:238–243.

43. Hedges TR Jr, Baron EM, Hedges TR III, Sinclair SH. The retinal venous pulse. Its relation to optic disc characteristics and choroidal pulse. *Ophthalmology*. 1994;101:542–547.

44. Schmoll T, Leitgeb RA. Heart-beat-phase-coherent Doppler optical coherence tomography for measuring pulsatile ocular blood flow. *J Biophotonics*. 2013;6:275–282.

45. Werkmeister RM, Palkovits S, Told R, et al. Response of retinal blood flow to systemic hyperoxia as measured with dual-beam bidirectional Doppler fourier-domain optical coherence tomography. *PLoS One*. 2012;7:e45876.

46. Lee B, Choi W, Liu J, et al. Cardiac-gated en face doppler measurement of retinal blood flow using swept source optical coherence tomography at 100,000 axial scans per second. *Invest Ophthalmol Vis Sci*. 2015;56:2522–2530.

47. Chen HC, Patel V, Wiek J, Rassam SM, Kohner EM. Vessel diameter changes during the cardiac cycle. *Eye*. 1994;8:97–103.

48. Kotliar KE, Vilser W, Nagel E, Lanzl IM. Retinal vessel reaction in response to chromatic flickering light. *Graefes Arch Clin Exp Ophthalmol*. 2004;242:377–392.

49. Schmoll T, Singh ASG, Frily K, et al. Flicker stimulated retinal perfusion changes assessed with high-speed Doppler tomography. *Proc SPIE*. 2010;7550:F1–F4.

50. Hao H, Sasongko MB, Wong TY, et al. Does retinal vascular geometry vary with cardiac cycle? *Invest Ophthalmol Vis Sci*. 2012;53:5799–805.

51. Silver DM, Farrell RA, Langham ME, O'Brien V, Schilder P. Estimation of pulsatile ocular

blood flow from intraocular pressure. *Acta Ophthalmol Suppl*. 1989;191:25–29.

52. Silver DM, Farrell RA. Validity of pulsatile ocular blood flow measurements. *Surv Ophthalmol*. 1994;38(suppl);S72–S80.

53. Michelson G, Harazny J. Relationship between ocular pulse pressures and retinal vessel velocities. *Ophthalmology*. 1997;104:664–671.

54. Jonas JB, Wang N, Yang D, Ritch R, Panda-Jonas S. Facts and myths of cerebrospinal fluid pressure for the physiology of the eye. *Prog Retin Eye Res*. 2015;46:67–83.

55. Westlake WH, Morgan WH, Yu DY. A pilot study of in vivo venous pressures in the pig retinal circulation. *Clin Experiment Ophthalmol*. 2001;29:167–170.

56. Taylor AW, Sehu W, Williamson TH, Lee WR. Morphometric assessment of the central retinal artery and vein in the optic nerve head. *Can J Ophthalmol*. 1993;28:320–324.

57. Williamson TH, Barr DB, Baxter GM. Understanding of the retinal circulation provided by an anomalous retinal vein. *Br J Ophthalmol*. 1994;78:798–799.

58. Williamson TH, Lowe GD, Baxter GM. Influence of age, systemic blood pressure, smoking, and blood viscosity on orbital blood velocities. *Br J Ophthalmol*. 1995;79:17–22.

59. Smith P. The blood-pressure in the eye and its relation to the chamber-pressure. *Br J Ophthalmol*. 1918;2:257–272.

60. Paques M, Garmyn V, Catier A, Naoun K, Vicaut E, Gaudric A. Analysis of retinal and choroidal circulation during central retinal vein occlusion using indocyanine green videoangiography. *Arch Ophthalmol*. 2001;119:1781–1787.

61. Paques M, Baillart O, Genevois O, Gaudric A, Levy BI, Sahel J. Systolodiastolic variations of blood flow during central retinal vein occlusion: exploration by dynamic angiography. *Br J Ophthalmol*. 2005;89:1036–1040.

62. Morgan WH, Hazelton ML, Betz-Stablein BD, et al. Photoplethysmographic measurement of various retinal vascular pulsation parameters and measurement of the venous phase delay. *Invest Ophthalmol Vis Sci*. 2014;55:5998–6006.

63. Atebara NH, Brown GC. Ocular ischemic syndrome. In: Tasman W, Jaeger EA, eds. *Duane's ophthalmology on CD-ROM edition*. Philadelphia: Lippincott, Williams, & Wilkins; 2006: Chapter 12.

64. Kommerell G. Schlängelung der Netzhauterien durch die Pulswelle. *Klin Monatsbl Augenheilkd*. 1978;173:486–488.

65. Newell FW. *Ophthalmology: Principles and Concepts*. St. Louis: CV Mosby; 1992.

66. Keyes JEI, Hatcher WF. The interpretation of visible pulsation in the retinal arteries. *J Am Med Assoc*. 1940;114:2089–2090.

67. Grosvenor T. *Primary Care Optometry*. St Louis: Elsevier Health Sciences; 2007.